

Effect of the seismic shaking and ejecta coverage erasure on the crater population of 433 Eros

Blitz, C. (1,2), Komatitsch, D. (2,3), Lognonné, P. (1), Martin, R. (3) and Legoff, N. (4)

(1) Équipe Géophysique Spatiale et Planétaire, CNRS UMR 7354, Institut de Physique du Globe de Paris et Université de Paris Diderot, 94100 Saint Maur des Fossés, France

(2) Université de Pau et des Pays de l'Adour, CNRS et INRIA Magique-3D, Laboratoire de Modélisation et d'Imagerie en Géosciences UMR 5212, Avenue de l'Université, 64013 Pau, France

(3) Institut Universitaire de France, 103 boulevard Saint-Michel, 75005 Paris, France

(4) Université de Pau et des Pays de l'Adour, INRIA Magique-3D, Laboratoire de Mathématiques appliquées, Avenue de l'Université, 64013 Pau, France

The crater population of asteroid 433 Eros displays a deficit in small crater sizes (Chapman et al., 2002) probably linked to erasure mechanism such as impact-induced seismic shaking (Richardson et al., 2005) which triggers downslope movements on crater walls (leading to bright tracks on Eros surface), electrostatic dust levitation leading to the formation of flat ponded deposits inside craters (Asphaug, 2004) and ejecta coverage process, burying the craters with impacts debris (Robinson et al., 2002). This study presents an erasure model including both the seismic shaking process and the ejecta coverage processes. The seismic shaking simulation is based on accurate wave propagation simulations performed with the powerful spectral-element method. This method, commonly used in Earth seismology, (Komatitsch and Tromp, 1999) is applied to a realistic 2-D model of asteroid Eros. The maximum acceleration computed will define the factor of safety on the crater walls and a geometrical model of downslope movement will be applied if the seismic vibrations are strong enough. This mobilized material can bury craters by filling them.

The ejecta coverage process is based on the ballistic study of ejecta trajectories around an ellipsoidal model of the asteroid Eros, leading to a regolith production rate. This rate will be applied to the crater to check if they can be buried by the regolith blanket accumulation. These two processes can probably act together; such scenario is simulated to infer the contribution of each erasure process on the crater deficit of asteroid Eros.

EJECTA COVERAGE MODELING

To simulate this process, an ellipsoidal model of asteroid Eros is impacted by a projectile population of the Main Asteroid Belt (O'Brien et al., 2006). From each projectile, a crater is created and ejecta blocks trajectories are studied around the ellipsoid. The falling of the ejecta leads to the regolith deposit, with a distribution shown in Figure 1 for an exposure time of 400 Myrs.

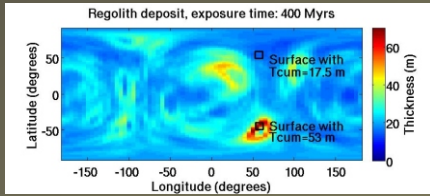


Fig. 1 - Distribution of the regolith created by each ejecta fall during an exposure time of 400 Myrs. 5,993,602 ejecta trajectories have been computed. The total average regolith thickness obtained is 26 m.

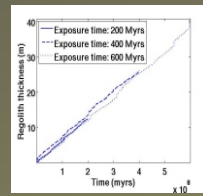


Fig. 2 - Average production rate of regolith during different exposure times

The first impacts of the cratering history of Eros are considered to occur on the asteroid bedrock (since no regolith has formed yet), so an excavation in a bedrock type material is simulated at these early times. When the regolith reaches about 3.7 m it is thick enough to allow cratering and excavation in a regolith target. Figure 2 shows that the simulations of ejecta accumulation lead to a linear average regolith production, with a slope $(T_{cum} / T_{exp}) = 7 \times 10^{-8} \text{ m.yr}^{-1}$. This production rate is slightly lower while the regolith thickness is smaller than 3.7 m; during these early times, the cumulative regolith thickness is created from a bedrock target, but this variation of the rate is negligible in the general trend. This linear rate is used for the regolith production in the impact-induced seismic shaking modelling and is also considered as an erasure mechanism. A crater is considered erased if one tenth of its diameter is covered by ejecta (Richardson et al., 2005).

Considering the single effect of ejecta coverage on the crater population of asteroid Eros, we observe (figure 3) that this process has an important contribution to crater erasure (in particular for the smallest craters), but it does not produce enough regolith to be the only phenomenon responsible for the observed deficit in the smallest crater sizes.

Fig. 3 - Cumulative size-frequency distribution plots of Eros craters per square kilometer as a function of crater diameter assuming the ejecta coverage erasure process

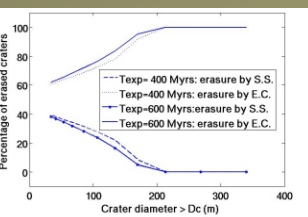
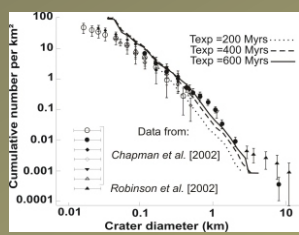


Fig. 11 - Contribution of the seismic shaking and ejecta coverage process on the erasure of craters for exposure times of 400 Myrs and 600 Myrs.

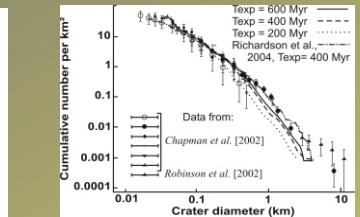


Fig. 10 - Cumulative size-frequency distribution plots of Eros craters per square kilometer as a function of crater diameter, displaying a best agreement between the observed and modeled populations after a Main Belt exposure time of 600 Myrs.

SEISMIC SHAKING MODELING

1- Wave propagation simulation

So as to quantify the effect of a seismic source like an impact on a crater (the source is represented by a filtered Dirac function in the present study), we performed seismic modeling to simulate the accelerograms at 45 different locations on the 2-D model of Eros (figure 4 and 5). The using method for simulation in seismology is the spectral element method (Komatitsch and Tromp, 1999). This numerical method consists in approximating the solution of linear elastodynamic equations (in the weak form) on a grid of the studied object. In the present simulations, the 2-D grid is discretized into quadrangles, inside which the numerical integration is based on the tensor product of a Gauss-Lobatto-Legendre 1-D quadrature. The solution is expanded onto a discrete polynomial basis so as to produce a diagonal mass matrix that reduces the computational cost. The wave propagation is studied at a dominant frequency of 2 Hz with a source intensity corresponding to a chondritic projectile of 50 m in diameter impacting Eros at 5300 m/s. The 2-D model of Eros includes a bed-rock simulated by an elastic material characterized by a pressure wave velocity $V_p = 3000 \text{ m.s}^{-1}$, a shear wave velocity $V_s = 2000 \text{ m.s}^{-1}$ and a density of 2700 kg.m^{-3} . This model is also characterized by cracks, ridge and regolith, simulated with a pressure wave velocity $V_p = 900 \text{ m.s}^{-1}$, a shear wave velocity $V_s = 500 \text{ m.s}^{-1}$ and a density of 2000 kg.m^{-3} .

3 - Downslope movements modeling

We have computed for crater sizes of 40m, 100m, 600m, 1000m, 3000m and 6000m the depth of regolith which fill the crater as a function of time. To do so, we have assumed that the downslope movement on craters slope is occurring only when the factor of safety is lower than one (this factor is linked to the crater slope, the cohesion of the regolith, the regolith thickness lying on the slope, the local gravity, and the maximum acceleration that will eventually destabilize the regolith blanket after an impact). For a given studied crater, the regolith blanket on the wall grows with the rate of $7 \times 10^{-8} \text{ m.yr}^{-1}$ (see ejecta coverage study), and each time the impact of a projectile reduces the factor of safety lower than one, a part of the regolith blanket slides downward to fill the bottom of the crater. This amount of sliding material depends on the projectile diameter. In order to estimate which depth of the crater is filled at each triggered downslope movement, we assumed a cap shape of the crater. The depth to which the mobilized material volume will fill the bottom of the crater is found with an iterative method, by equalizing the volume of the filled bottom of the crater, V_{bottom} (figure 8) with the volume of the mobilized material blanket, $V_{blanket}$ (figure 8). The iteration is made on the R2 diameter (that separate the two volumes). Knowing the R2 value allowing $V_{bottom} \sim V_{blanket}$, we can extract the depth value h , to which the crater interior is filled by the mobilized material. The successive downslope movements will produce superposed layers on the cap shape crater bottom that will progressively fill the cavity interior. When the regolith depth is higher than one tenth of its diameter D_c , the crater is considered as erased (Richardson et al., 2005). From this, we can estimate the life time of the six studied crater sizes which define a law:

$$\text{Life time} = 128487 \times D_c^{0.4906}$$

The combination of the two erasure processes have been performed by adding to the life-time condition of the craters (for the seismic shaking erasure process), a condition on the regolith infilling of the crater during time. If the regolith blanket that grows to a rate of $7 \times 10^{-8} \text{ m.yr}^{-1}$ is thicker than a tenth of the crater diameter, the crater is erased by the ejecta coverage process. By mixing the ejecta coverage and seismic shaking, we obtain an erasure process more efficient than one of these two processes alone (see figure 3 for ejecta coverage). We have compared the simulated crater populations (with the seismic shaking and ejecta coverage process) to the crater population obtained from the NEAR spacecraft data. The figure 10 suggests a best agreement between the data and the simulations for an exposure time $T_{exp} = 600 \text{ Myr}$, close to the value of 400 Myr obtained by Richardson et al., 2005. The figure 11 displays the contribution of the seismic shaking and ejecta coverage on the erasure of the crater population of Eros. We can see that the seismic shaking can bury craters with diameters lower than 210 m, but for all the crater sizes, ejecta coverage seems to be a more efficient process. This study suggests the occurrence of both seismic shaking and ejecta coverage erasure processes to explain the shape of the crater population of asteroid Eros.

2- Law of maximum accelerations

We assume that only the maximum accelerations triggered by an impact will affect a given crater. This assumption is realistic because after a big downslope movement (triggered by a very high acceleration) has occurred on a crater wall, a very small amount of material is remaining on the crater slope, then following regolith slumpings are less numerous. We performed five wave propagation simulations with five different source positions (figure 6). For each recorder of the five simulations, the maximum accelerations of signals are plotted as a function of the minimum distance source-recorder (figure 7).

Fig. 7 - Curve of the maximum acceleration as a function of the distance source-recorder

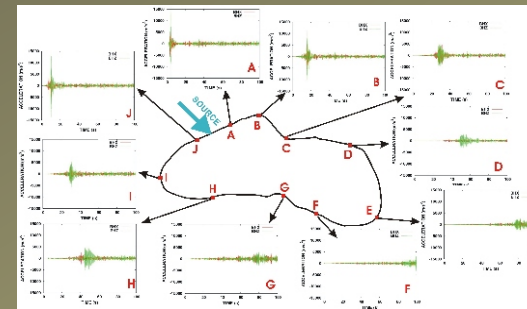


Fig. 4 - Seismograms in acceleration obtained with a source corresponding to an impact of a chondritic projectile of 50.5 m in diameter at a velocity of 5300 m/s (we show 10 synthetics out of 45)

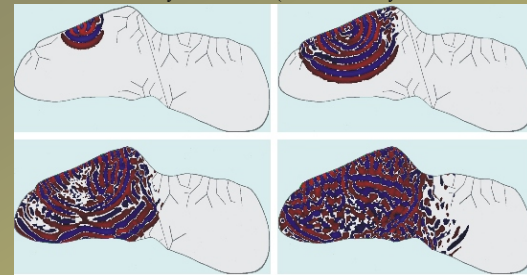


Fig. 5 - Snapshots in the vertical component of the displacement vector shown at times 1.5 s, 3 s (top), 4.5 s, 6.7 s (bottom).

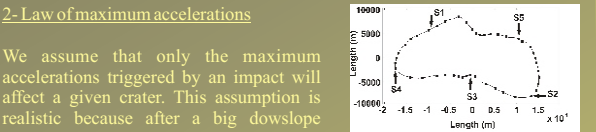
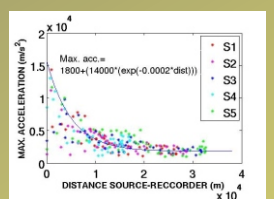
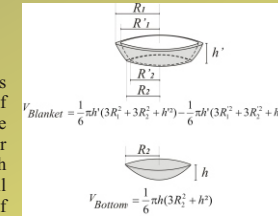


Fig. 6 - Location of the 5 sources used to create the curve of the maximum acceleration as a function of the distance source-recorder



Each impactor hitting Eros (characterized by its mass and its constant impact velocity) is considered as a different seismic source amplitude producing its own acceleration curve, but shifted upward or downward of the reference curve given in figure 7. Knowing each falling position of the impactors on the asteroid model (these location are chosen randomly on Eros surface), the distances between a given crater and the different impacts following its formation are computed. Informations about 1) the distance between the crater to the following impact and 2) the ratio of the impact momentum (between a given projectile and the reference projectile of 50.5 m in diameter), allows us to quantify the maximum acceleration a given crater is subjected to for each following impact.



$$V_{blanket} = \frac{1}{6} \pi h' (3R_1^2 + 3R_2^2 + h'^2) - \frac{1}{6} \pi h' (3R_2^2 + 3R_2^2 + h'^2)$$

$$V_{bottom} = \frac{1}{6} \pi h (3R_2^2 + h^2)$$

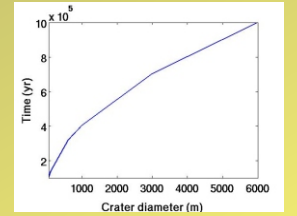


Fig. 8 - Schemes of the assumed calotte shape of craters for infilling laws. The filled bottom of a crater has a volume V_{bottom} and the blanket of the regolith lying on the crater wall has a volume $V_{blanket}$.

Fig. 9 - Life-time of craters as a function of their sizes. Although largest craters fill faster than small craters, they have to bury a thicker depth for being erased. From this, the large craters live longer unerased than small craters.